COARCTATION-INDUCED ABDOMINAL AORTIC ANEURYSM IN A PORCINE MODEL

Lin, P. Y[1,2,3]., Y. T. Wu[4], G. C. Lin[4,5], Y. H. Shih[5], A. Sampilvanjil[4], L. R. Chen[6], Y. J. Yang[3], H. L. Wu[2,7] and M. J. Jiang[2,4,*].

Institute of Clinical Medicine[1], Cardiovascular Research Center[2], Department of Cell Biology and Anatomy[4], Institute of Basic Sciences[5], and tDepartment of Biochemistry and Molecular Biology[7], National Cheng Kung University College of Medicine; the Department of Surgery, Division of Cardiovascular Surgery, National Cheng Kung University Hospital[3], Tainan 70101, Taiwan.
Physiology Division, Taiwan Livestock Research Institute, Tainan 71246, Taiwan[6]
*Corresponding author, e-mail: mjiang@mail.ncku.edu.tw, Tainan, 70101.

ABSTRACT

Hemodynamic stress participates in the initiation and progression of aneurysmal degeneration. Coarctation increases flow-mediated stress on the aortic wall. We tested the hypothesis that prolonged coarctation of an infrarenal abdominal aorta (AA) segment leads to abdominal aortic aneurysm (AAA) formation in mini pigs. An infrarenal AA segment of Taiwanese Lanyu mini pigs was wrapped with an 8 mm-wide ePTFE Teflon strip to create a funnel-shaped flow-path with constrictive outlet for 4 weeks (4 w), 8 weeks (8 w), and 12 weeks (12 w). This treatment resulted in moderate coarctation, manifested by pulsatility index reduced to one third the inherent levels, increased downstream flow-mediated stress and induced significant flow disturbance. Sham control pigs received Teflon wrapping without coarctation. Aneurysm characterized by progressive medial degeneration occurred at the terminal AA after 12 w coarctation. The outer dimension of the distal AA increased 50% compared to that of the proximal AA at 4 w, 8 w, and 12 w post-coarctation. Lumen ratio of the distal-to-suprarenal AA increased time-dependently with 12 w post-coarctation exhibiting significant increase. In the distal AA, elastic lamellae exhibited fragmentation at 4w and more pronounced fragmentation with decreased density at 8 w and 12 w post-coarctation. Smooth muscle exhibited disarray and nuclear density decrease at 8 w and 12 w post-coarctation. Gelatin zymography results showed that matrix metalloproteinase-9 activity markedly increased at 4 w post-coarctation. These results indicate that prolonged moderate coarctation caused regional hemodynamic stress and thereby induced degenerative AAA in the terminal AA.

Keywords: Abdominal aortic aneurysm, Coarctation, Hemodynamic stress, Porcine model

INTRODUCTION

Abdominal aortic aneurysm (AAA) is a life-threatening disease that affects 4 to 8 % of the population over 65 years of age (Nordon *et al*., 2011). The disease process mainly occurs at the infrarenal abdominal aortic (AA) segment, where gradual weakening and dilatation of the aortic wall develop as the consequences of chronic structural degeneration (Longo *et al*., 2002). AAA usually remains asymptomatic prior to the catastrophy of rupture, which has over 80 % risk of death (Verhoeven *et al*., 2008). Currently, AAA treatment focuses on avoiding aneurysm rupture. Changing strategy from passively preventing rupture to actively reducing degeneration should help improve outcomes of AAA treatment (Wassef *et al*., 2007).

Reducing aneurysm degeneration relies on thoroughly understanding the pathogenesis of AAA. Along AAA degeneration, aneurysmal wall is characterized by progressive destruction of extracellular matrix (ECM) and loss of vascular smooth muscle cells (VSMC). The destruction of ECM, resulting from excessive proteolytic degradation, leads to decreased tensile strength. When wall stress exceeds the tensile strength, aneurysm rupture occurs (Vorp and Vande Geest, 2005). Identifying the pathophysiological factors that facilitate destruction of the vascular wall should help develop new diagnostic and therapeutic modalities for AAA.

To gain insight into the pathogenesis of AAA development, an animal model mimicking early human aneurysmal degeneration is needed. We hypothesized that prolonged coarctation at the infrarenal AA segment induces outward vascular remodeling and consequently leads to AAA formation. The aneurysm degeneration was simulated in porcine AA with coarctation that creates flow disturbance and increases hemodynamic stress on the aortic wall.

MATERIALS AND METHODS

Animals

Taiwanese Lanyu mini pigs, 7-10 months-old adults consisting of both genders, were provided by Taitung Animal Propagation Station of the Taiwan Livestock Research Institute and completed the quarantine before experiments. Thirty mini pigs were randomly divided into six groups: three experimental groups (7 pigs/group) undergoing aortic coarctation for 4 weeks (4 w), 8 weeks (8 w), and 12 weeks (12 w) and sham groups (3 pigs for each time point) as the control. The whole study conforms to the *Guide for the Care and Use of Laboratory Animals* published by the National Institute of Health (U. S. A.) and the experimental procedures were approved by the institutional Animal Care and Use Committee.

Anesthesia and Aortic Coarctation

Preanesthesia induction of mini pigs was conducted by intramuscularly injecting a

mixture of tranquilizer, analgesics and anticholinergics containing Zoletil 50 (10 mL), Rompun (5 mL) and atropine (1 mL) at pigs' gluteal region. The sedative pigs were placed on the operation table with supine position and intravenous fluid infusion routes were established through the postauricular veins. Endotracheal intubation was performed and isoflurane (2 % of the tidal volume) was continuously given during surgery to maintain general anesthesia. To better expose infrarenal aorta and bilateral common iliac arteries, trans-peritoneal cavity approach via laparotomy was taken. After opening the retroperitoneum, infrarenal AA was isolated free from the surrounding tissues. An ePTFE Teflon strip with 8-mm-diameter to simulate infrarenal AA size was used to encircle the AA approximately 2 cm above the aortic bifurcation. The Teflon strip was tailored to a funnel-shaped tube which modeled the wrapped aortic segment into a tapered channel with nonconstrictive inlet and constrictive outlet (Figure 1A). Sham group received retroperitoneal opening, AA isolation, and Teflon strip wrapping without aortic coarctation. The surgical procedure was carried out under aseptic conditions and completed within three hours to avoid respiratory distress caused by prolonged supine posture.

Quantitative Characterization of Aortic Coarctation

To achieve moderate coarctation, we used pulsatility index to quantitatively characterize hemodynamic changes. Pulsatility index was calculated by dividing the difference between the maximal and minimal flow rate with the mean flow rate (Beldi *et al*., 2000). The decrease in pulsatility index is proportional to the extent of aortic coarctation (Silvilairat *et al.*, 2008). Our criteria for moderate coarctation were pulsatility index reduced to one-third inherent level (Figure 1B) combined with turbulent flow in the aortic segment distal to constriction (Figure 2A). Transit time flowmeter system (Medi-Stim VeriQ system, Oslo, Norway) was used during operation to simultaneously monitor flow, pressure, and pulsatility index changes at both the proximal and distal AA segments of the coarctation. Flow turbulence was detected by duplex ultrasound scanning (MicroMaxx, SonoSite Inc. USA).

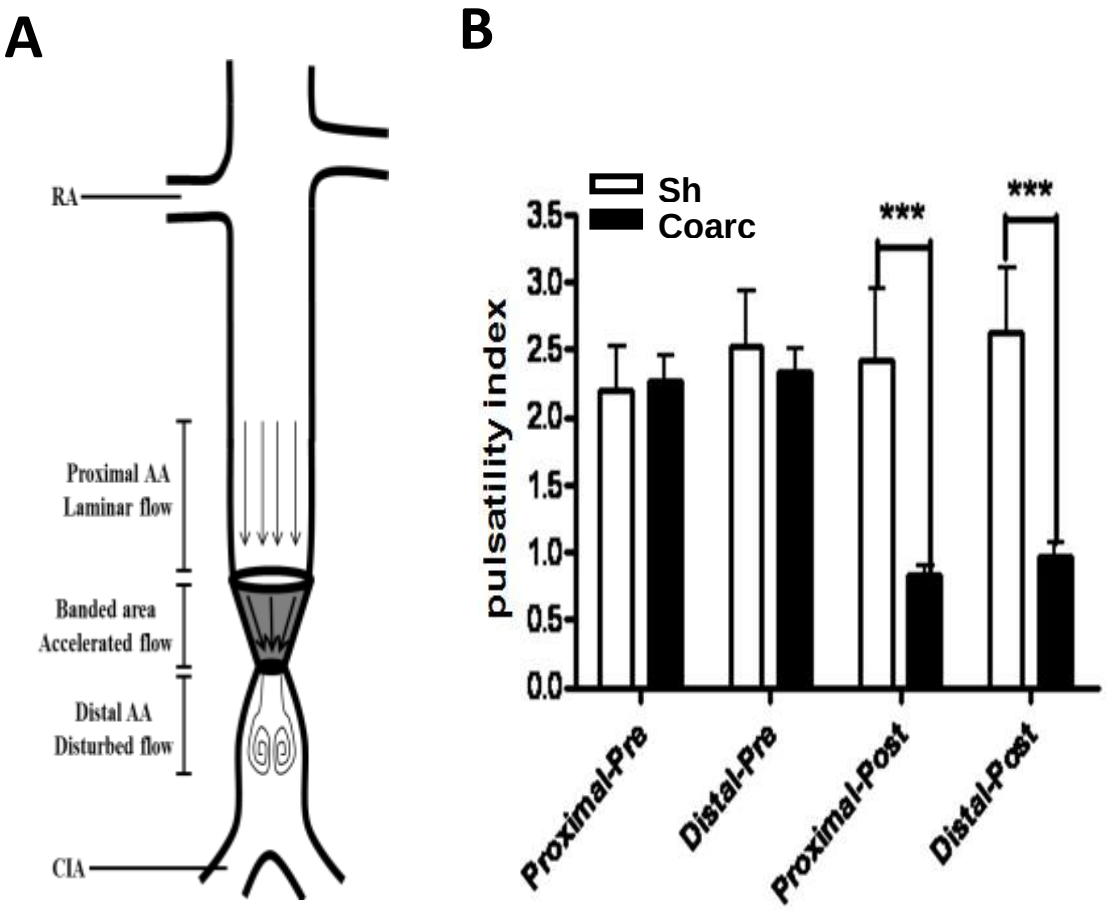

Figure 1. Coarctation decreased pulsatility index in both proximal and distal AA segments. A illustrates the location of coarctation at an infrarenal AA segment approximately 2 cm proximal to the aortic bifurcation**.** An 8 mm-long ePTFE strip was used to encircle an AA segment with a non-constrictive inlet and a constrictive outlet. **B** summarizes pulsatility index at the regions proximal and distal to the coarctation. Values were expressed as mean ± SEM (sham, n = 4; coarctation, n = 8), *** $P < 0.005$. CIA, common iliac artery; RA, renal artery. (reproduced from Lin *et al*., 2013)

Sacrifice and Tissue Processing

Mini pigs were anesthetized as described in the coarctation operation. Before the retroperitoneum was opened, duplex ultrasound scanning was performed to acquire images of the aortic lumen at the distal AA segment. After infrarenal AA was isolated, blood flow, PI, and intraluminal blood pressure at the proximal and distal AA segments were monitored. In addition, the outer diameter of various AA segments was measured. Animals were then sacrificed with an intravenous injection of KCl (2 mmol/kg body weight). AA segments from the regions proximal and distal to the coarctation, and suprarenal area were collected. Tissues were fixed in 4 % buffered paraformaldehyde, dehydrated with sequential incubation with ethanol from 70 % to 100 %, cleared with xylene, and embedded with paraffin.

Histological Examination of the Abdominal Aorta

To examine the overall morphology and the distribution of the elastic lamellae and collagen fibers in various AA segments, hematoxylin-and-eosin (H&E), Verhoeff Van Gieson and Masson's trichrome staining were performed. Paraffin sections (4 μm thick) were deparaffinized, rehydrated, and stained according to the manufacturer's instructions.

Detecting Smooth Muscle Density with Immunohistochemistry

Paraffin sections were processed and incubated overnight with monoclonal antibody against smooth muscle-specific α-actin (1 : 400, clone E 184, Epitomics) at 4 ℃. Aortic sections were subsequently incubated with either horseradish peroxidase-conjugated horse anti-mouse immunoglobulin and chromogen substrate or with Alexa 594-conjugated horse anti-mouse immunoglobulin and Hoechst 33342.

Quantification

The aortic lumen perimeter, medial smooth muscle percent area, and medial nuclear density were measured by Image Pro-Plus. The relative abundance of collagen and elastic fibers in the media was quantified using a published method (Hu et al., 2008) in four sections with 80 μm intervals and 4 fields (100x magnification) each.

Gelatin Zymography

Gelatin zymography was performed according to a published report (Davis et al., 1998). Briefly, the AA samples were powdered in liquid nitrogen, homogenized, and extracted twice in TNC buffer containing 50 mM Tris base, 150 mM NaCl, 10 mM $CaCl_2$, 0.05 % Brij 35 and 0.02 % NaN3, twice in TNC buffer containing 2 % DMSO, and once in TNC buffer containing 10 M urea. Aortic homogenates were separated with SDS-polyacrylamide gel electrophoresis containing 0.1 % gelatin under non-reducing condition at 4 ℃. Gels were re-natured, developed for 16 h at 37 ℃, stained with Coomassie blue, and destained until clear bands were detected. Gelatinolytic activity was analyzed with densitometry.

Statistical Analysis

Data are expressed as means ± SEM; *n* is the number of pigs. The data were analyzed first with one-way ANOVA, followed by Tukey's Honestly Significant Difference test between groups. Statistical significance was set at $P < 0.05$.

RESULTS AND DISCUSSION

Changes in Blood Pressure and Pulsatility Index

We measured blood pressure at the AA segments proximal and distal to the coarctation site after operation and before sacrifice in 12 pigs. Following coarctation, systolic blood pressure (SBP) at the distal AA decreased and a pressure gradient of approximately 30 mmHg was detected between the proximal and distal AA segments. In contrast, diastolic blood

pressure (DBP) did not vary between these AA segments. Interestingly, both SBP at the distal AA and PI values were back to the pre-operation levels at sacrifice.

Coarctation Induced AAA Formation in Mini Pigs

To determine whether coarctation induced aneurysm, we examined both the luminal and the outer diameters of the infrarenal AA segments before sacrifice and measured the luminal perimeters of the distal AA segments in cross sections. The luminal diameters, examined with duplex ultrasonography following the opening of the retroperitoneum, showed that the distal AA segment at 12 w post-coarctation exhibited pronounced dilatation whereas that of the sham group was near constant in size (Figure 2B). The outer diameter of the distal AA segment markedly increased at 4 w post-coarctation and maintained similar size up to 12 w post-coarctation (sham: 1.0 ; 4 w: 1.7 ± 0.08; 8 w: 1.5 ± 0.09; 12 w: 1.7 ± 0.01). H&E staining showed that the lumen perimeter ratio of the distal-to-suprarenal segment didn't change at 4 w, increased at 8 w, and reached approximately 50 % at 12 w post-coarctation (4 w: 1.1 ± 0.11, n = 5; 8 w: 1.4 ± 0.20, n = 6; 12 w: 1.5 ± 0.09, n = 7; sham: 1.0 ± 0.05, n = 9). These results showed that hemodynamic forces participate in the evolutionary degeneration process. Through constricting an infrarenal AA segment, we created a disturbed flow environment at the distal region where oscillatory shear stress was pronounced. Consequently, AAA developed and aneurysm degeneration continued to evolve under the persistent impact of regional pathological hemodynamics. We noted that the adjacent position of the coarctation site to the aortic bifurcation, approximately 2 cm apart, appeared to facilitate aneurysm formation. This may result from more pronounced flow disturbance that is consistent with the low/oscillatory shear stress and increased pulse wave reflection/wall strain detected near aortic bifurcation, which increase aneurysm susceptibility of the site (Humphrey and Taylor, 2008).

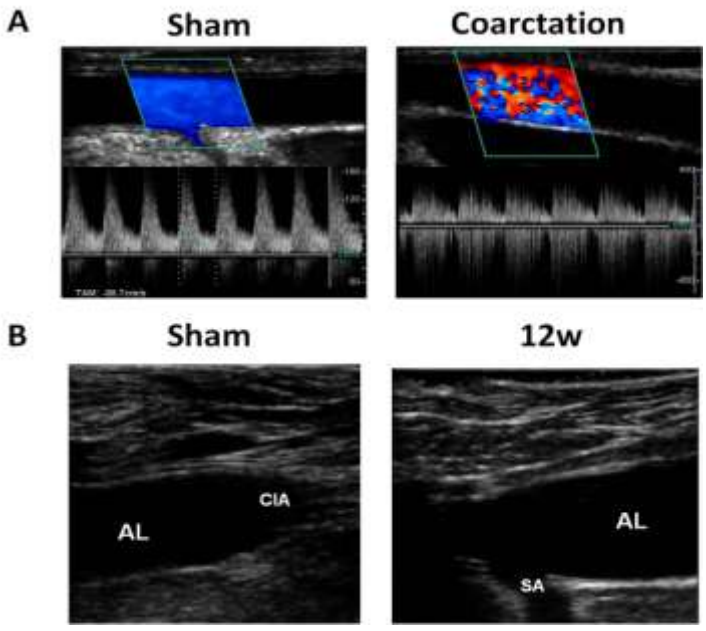

Figure 2. Coarctation induced turbulent flow and aneurysm in the distal AA segment.

Duplex ultrasonography was conducted during the coarctation procedure and before sacrifice to moniter the flow patterns in the distal AA segment. **A**, ultrasonographic images showed a mosaic flow pattern with decreased peak systolic flow and increased reverse flow after coarctation and lamellar flow pattern in sham

control. **B**, dilatation of distal AA segment after 12 w coarctation. AL, aortic lumen; CIA, common iliac artery; SA, spinal artery. (reproduced from Lin *et al*., 2013)

Distal AA Segment Exhibits Structural Characteristics of AAA

To characterize the structural changes in the AA wall, we examined the density of elastic lamellae and collagen fibers. In the distal AA, elastic lamellae in the media showed no change in density at 4w post-coarctation, but exhibited pronounced decrease and fragmention at 8 w and 12 w post-coarctation (percent area of elastic fibers in the media, sham: 2.8 ± 0.56%, n = 7; 4 w: 3.0 ± 0.25 %, n = 8; 8 w: 1.9 ± 0.31 %, n = 8; 12 w: 1.0 ± 0.23 %, n = 4). In contrast, no change in the density of collagen fibers was detected (data not shown). The destruction of elastic lamellae is a well recognized characteristic of aortic aneurysm both in patients and in experimental AAA. To further clarify the mechanisms responsible for elastic fiber destruction, we examined the expression and activity of matrix metalloproteinase (MMP)-2 and MMP-9, two MMPs reported to play important roles in AAA formation (Davis *et al*., 1998, Longo *et al*., 2002). MMP-2 exhibited high intrinsic activity and expression levels which didn't increase after coarctation (data not shown). In contrast, proMMP-9 activity and expression exhibited the trend to increase in the coarctation groups compared to the sham control and was significantly upregulated at 4 w post-coarctation. Because multiple MMPs were reported to be involved in aneurysm formation, we are looking into changes in the expression levels of MMPs and tissue inhibitors of MMPs (TIMPs) during AAA formation.

To examine whether changes occurred in VSMC during AAA formation, we measured the area and calculated nuclear density in the media. While no change in percent area was detected, nuclear density of the media markedly decreased at 8w and 12w post-coarctation (sham: 6966 ± 888/mm^2; 4 w: 5747 ± 1340/mm^2; 8 w: 4153 ± 323/mm^2; 12 w: 4083 ± 465/mm^2). These results suggested that VSMC hypertrophy occurred during AAA progression. It's interesting to note that in some medial area near the adventitia, the alignment of VSMC appeared to change from circularly oriented, highly ordered layers into longitudinally or obliquely oriented bundles at 8 w and 12 w post-coarctation. Furthermore, the boundary between media and adventitia was difficult to define in some areas. These phenomena, in combination with the upregulated MMP-9 activities, provided strong indication for extensive remodeling during AAA formation and progression. We are currently examining changes in VSMC phenotype and the interplay among vascular cells and infiltrated inflammatory cells.

REFERENCES

Beldi, G., A. Bosshard, O. M. Hess, U. Althaus, and B. H. Walpoth. 2000. Transit time flow measurement: Experimental validation and comparison of three different systems. Ann.

Thorac Surg. 70:212-217.

Davis, V., R. Persidskaia, L. Baca-Regen, Y. Itoh, H. Nagase, Y. Persidsky, A. Ghorpade, and B. T. Baxter. 1998. Matrix metalloproteinase-2 production and its binding to the matrix are increased in abdominal aortic aneurysms. Arterioscler Thromb. Vasc. Biol. 18:1625-1633.

Hu, J. J., A. Ambrus, T. W. Fossum, M. W. Miller, J. D. Humphrey, and E. Wilson. 2008. Time courses of growth and remodeling of porcine aortic media during hypertension: A quantitative immunohistochemical examination. J. Histochem. Cytochem. 56:359-370.

Humphrey, J. D., and C. A. Taylor. 2008. Intracranial and abdominal aortic aneurysms: Similarities, differences, and need for a new class of computational models. Annu. Rev. Biomed. Eng. 10:221-246.

Lin, P. Y., Y. T. Wu, G. C. Lin, Y. H. Shih, A. Sampilvanjil, L. R. Chen, Y. J. Yang, H. L. Wu, and M. J. Jiang. 2013. Coarctation-induced degenerative abdominal aortic aneurysm in a porcine model. J. Vasc. Surg. 57:806-815 e801.

Longo, G. M., W. Xiong, T. C. Greiner, Y. Zhao, N. Fiotti, and B. T. Baxter. 2002. Matrix metalloproteinases 2 and 9 work in concert to produce aortic aneurysms. J. Clin. Invest. 110:625-632.

Nordon, I. M., R. J. Hinchliffe, I. M. Loftus, and M. M. Thompson. 2011. Pathophysiology and epidemiology of abdominal aortic aneurysms. Nat. Rev. Cardiol. 8:92-102.

Silvilairat, S., F. Cetta, G. Biliciler-Denktas, N. M. Ammash, A. K. Cabalka, D. J. Hagler, and P. W. O'Leary. 2008. Abdominal aortic pulsed wave doppler patterns reliably reflect clinical severity in patients with coarctation of the aorta. Congenit. Heart Dis. 3:422-430.

Verhoeven, E. L., M. R. Kapma, H. Groen, I. F. Tielliu, C. J. Zeebregts, F. Bekkema, and J. J. van den Dungen. 2008. Mortality of ruptured abdominal aortic aneurysm treated with open or endovascular repair. J. Vasc. Surg. 48:1396-1400.

Vorp, D. A., and J. P. Vande Geest. 2005. Biomechanical determinants of abdominal aortic aneurysm rupture. Arterioscler Thromb. Vasc. Biol. 25:1558-1566.

Wassef, M., G. R. Upchurch, Jr., H. Kuivaniemi, R. W. Thompson, and M. D. Tilson, 3rd. 2007. Challenges and opportunities in abdominal aortic aneurysm research. J. Vasc. Surg. 45:192-198.